

Synergistic Adsorption of N-dodecyl Ethylenediamine Along with Polyethylene Glycol (PEG) on Quartz

Wengang Liu*, Xinyang Wang, Wenbao Liu, Dezhou Wei, Benying Wang, Yanbai Shen

College of Resources and Civil Engineering, Northeastern University, Shenyang, Liaoning, China

*E-mail: liuwengang@mail.neu.edu.cn

Received: 24 July 2015 / Accepted: 19 August 2015 / Published: 30 September 2015

With the purpose of investigating the synergistic adsorption of polyethylene glycol (PEG) and N-dodecyl ethylenediamine (ND) on quartz surface, froth flotation accompanying with zeta potential measurements, FTIR studies, SEM/EDS analysis and molecular dynamics simulations were conducted in laboratory. Flotation results indicated that quartz flotation recovery could be improved significantly by the addition of PEG using ND as collector. The highest flotation recovery of quartz could be obtained when ND and PEG were mixed at a mass ratio of 1:1. Synthetic mixture of hematite and quartz could be separated at neutral slurry pH. Zeta potential measurements, FTIR analyses and SEM-EDS studies revealed the co-adsorption of PEG along with ND on quartz surface. The addition of PEG strengthened the electrostatic and hydrogen bond adsorption between quartz and collector. Furthermore, molecular dynamics simulations revealed the even stronger adsorption between ND/PEG mixture and quartz compared with ND or PEG adsorb individually.

Keywords: Synergistic adsorption; N-dodecyl ethylenediamine; PEG; Quartz; Zeta potentials

1. INTRODUCTION

Froth flotation is viewed as the most effective method to recover valuable minerals from gangue in mineral separation process. During this process, separation of minerals is achieved for selective adsorption of collectors on wanted mineral surface to render it hydrophobic. Conventionally, hydrophobic minerals that attach to air bubbles in stirred vessel are recovered once the froth overflows the weir. Conversely, hydrophilic minerals remain in liquid phase for they can not attach to the bubbles and then being removed as tailing fraction [1–4]. During flotation separation process, flotation reagents play a key role. The selectivity of collector is crucial to achieve high quality concentrate accompanying with great recovery in mineral separation [5].

Quartz, which is the main gangue mineral exist in iron ores, is frequently floated with cationic collectors. And such collectors as fatty primary alkylamines, coco amine, tallow-amine, ether amines and quaternary ammonium surfactant have been widely used both from technological and economical points [1,6–10]. However, most of these cationic surfactants have such shortcomings as high cost, cohesive bubble and poor selectivity [11].

Meanwhile, many studies have indicated that when more than two collectors are used in flotation process, greater recovery for valuable mineral(s) can be obtained than proportional contribution of each one, and then the collectors are purported to be acting synergistically [12]. Many investigators have demonstrated the improvement of silicate cationic flotation with the addition of non-ionic surfactants, as well as a significant reduction in cationic collector consumption [13–15]. Filippov et al. [6,17] showed that adding iso-alcohols to dodecylamine or ether diamine can improve quartz and Fe-bearing mica mineral floatability, while reducing the amine consumption. The role of long-chain alcohols in mixed amine-alcohol system on amine adsorption on quartz surface was to reduce the electrostatic repulsive force of dodecylamine cations in adsorption layer [14,15].

Polymers, which have gigantic molecules, have been widely used in flotation as flocculants [18], collectors [19] and depressants [20,21]. However, few reports are available regarding the use of mixtures containing diamine and polymer during the flotation of quartz and other silicates at present, and few works have focused on utilization of polyethylene glycol (PEG) in flotation. Thus, the purpose of this paper is to discuss the role of PEG in quartz flotation system with diamine collector. And the underlying synergistic adsorption mechanism of diamine along with PEG on quartz surface is also illustrated.

2. MATERIALS AND METHODS

2.1. Materials

Handpicked minerals (quartz and hematite) were collected from Qidashan plant located in Liaoning province, China. The quartz was crushed and then ground in one laboratory porcelain mill. The hematite was prepared by stage crushing and grinding in one stainless ball mill at a solid concentration of 70% in distilled water. The samples with the size below 0.100 mm were classified and used for further studies. Chemical compositions of the samples were given in Table 1.

Table 1. Chemical analyse results of the samples (mass fraction, %).

Species	TFe	SiO ₂	Al ₂ O ₃	CaO
hematite	69.69	0.25	0.02	0.07
quartz	0.21	99.50	0.06	0.09

Mineralogical analyses of the samples were conducted using a Shimadzu XRD-6100 powder diffractometer with a 92 Cu/K α X-ray source at 40 kV and 40 mA. The X-ray analysis results were

shown in Figure 1, which indicated that the primary minerals contained in sample were quartz and hematite. The sample was ground to $-10\mu\text{m}$ in a mortar mill for zeta-potential and FTIR studies. The above-mentioned results showed the purities of prepared hematite and quartz were 99.55% and 99.50%, respectively. Hematite and quartz were mixed at a proportion of 3:2 to compose the synthetic feed materials.

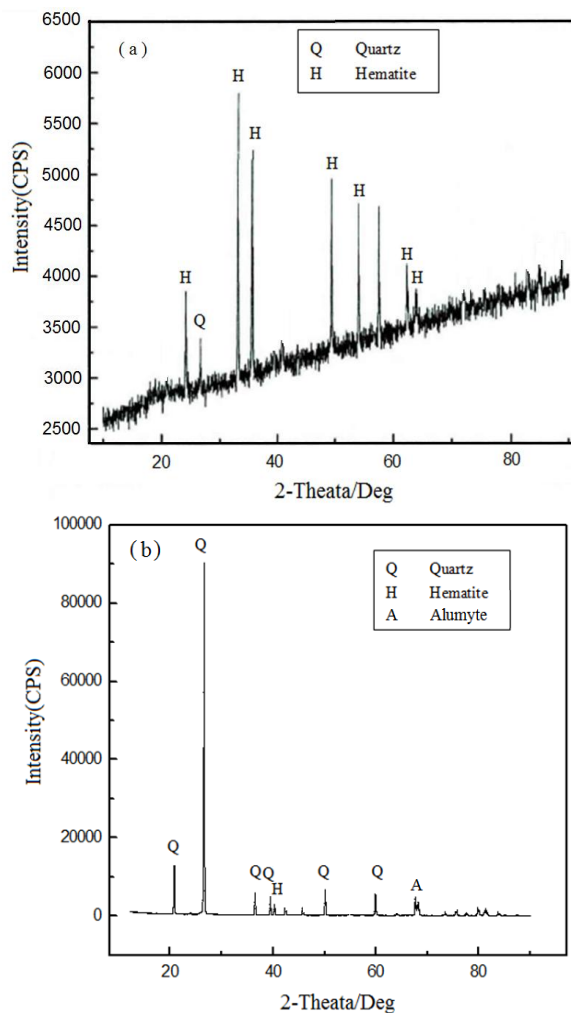


Figure 1. X-ray diffraction pattern of hematite (a) and quartz (b).

N-dodecylethylenediamine (ND) was synthesized in laboratory according to the procedure reported by Liu et al. [22] and used as such without any further purification. It was used in flotation as 1% mass concentration acetate solution. The analytical grade PEG-2000, which had an average molecular weight of 1800–2200, was purchased from Sinopharm, China. PEG was dissolved in distilled and deionized water which had an internal specific resistance of $18.2\text{ M}\Omega$ to form 1% mass percent concentration of PEG solution. ND/PEG solution was prepared by mixing ND solution with PEG solution together. Soluble starch of laboratory grade was prepared by dissolving it in slightly warm water and used as iron depressant. Dilute NaOH and HCl solutions were used to adjust the system pH.

2.2. Flotation tests

Flotation tests of quartz and hematite–quartz mixed sample were carried out in a 30 ml XFG–type flotation cell. Prepared mineral particles (5g) were put into a plexiglass flotation cell and suffused with deionized water. And then the suspension was stirred for 3 min by a plastic stirrer with four blade rotating at 1260 rpm. Then, starch and collectors were added into the flotation cell orderly with 3 min interval of conditioning time. Finally, the concentrate and tailing were collected separately, and then dried, weighted and assayed to determine the recovery and grade.

2.3. Zeta potential measurements

Zeta potentials of quartz were determined using a zeta plus analyzer (JS94H). Finely ground quartz ($-5\mu\text{m}$, 1g) were distributed in 50 mL 1×10^{-3} mol L⁻¹ KNO₃ aqueous solution and adjusted for 12 min at room temperature (25 °C). After pH of suspension was fixed to the desired value by HCl or NaOH, quartz zeta potentials (before and after being treated with collector) were measured. Then, an average value at least five individual measurement was accredited.

2.4. FTIR spectroscopy analysis

The infrared spectra were obtained using a Nicolet 740 FTIR spectrometer in the range of 400–4000 cm⁻¹. A pellet composed of a mixture of 100 mg KBr and 1mg sample was provided for studies. In order to demonstrate the nature of species adsorbed in quartz–aqueous solution interface, quartz particles were put in touch with aqueous solution of ND and ND/PEG mixture with a concentration of 33.33 mg L⁻¹ for 20 min. Then, quartz particles were separated by filtration, fully rinsed with deionized water and dried at 20°C for further investigation.

2.5. SEM/EDS studies

The surface morphology and composition of the sample before and after being treated with collectors were observed with a FESEM apparatus (JEOL JSM–6700F) furnished with an energy dispersive X–ray spectrometer (EDS) [23]. The operating voltage of FESEM was 5 kV.

2.6. Molecular dynamics simulations

Besides experimental methods, comparative performance of mixed collector for quartz was also investigated via molecular modeling calculations. The adsorption behavior of collectors on quartz surface was modeled using force field method. Here, the universal force field (UFF) was chosen to simulate quartz–collector in Materials studio 6.1 [24,25]. And a surface slab with depth of three layers was created from the unit cell of quartz crystal. The surface slabs, PEG molecule and ND molecule were also optimized using UFF as implemented in MS. In view of the importance of quartz surface

hydroxyl groups in aqueous flotation system, the surface oxygen atoms of quartz crystal were hydrogenated.

The simulated procedures were conducted according the report of Hu [26]. The total interaction energy with surfactant molecule over the mineral surface could be quantified and calculated in accordance with Eq. (1):

$$\Delta E = E_{complex} - (E_{surface} + E_{adsorbate}) \quad (1)$$

where $E_{complex}$ was the total energy of the adsorbate (collector) with the optimized mineral surface, $E_{surface}$ and $E_{adsorbate}$ were the total energies of bare quartz surface and adsorbate molecules, respectively. It is noteworthy that more negative adsorption energy implies more favorable interactions between mineral surface and adsorbate molecule. However, positive interaction energy (ΔE) reflects less favorable adsorption of adsorbate on mineral surface [24].

The simulation calculation was performed at 298 K, NVT ensemble. A time step of 0.1 fs was used and total simulation time of 5 ps was used for the equilibration run.

3. RESULTS AND DISCUSSION

3.1. Effect of PEG on quartz flotation

3.1.1 Pure quartz flotation

Figure 2 illustrated comparative studies on flotation performance of pure quartz when ND, PEG or ND/PEG mixture was used as collectors at pH 6-7. During flotation process, collector concentration was varied from 6.67mg L⁻¹ to 26.67 mg L⁻¹.

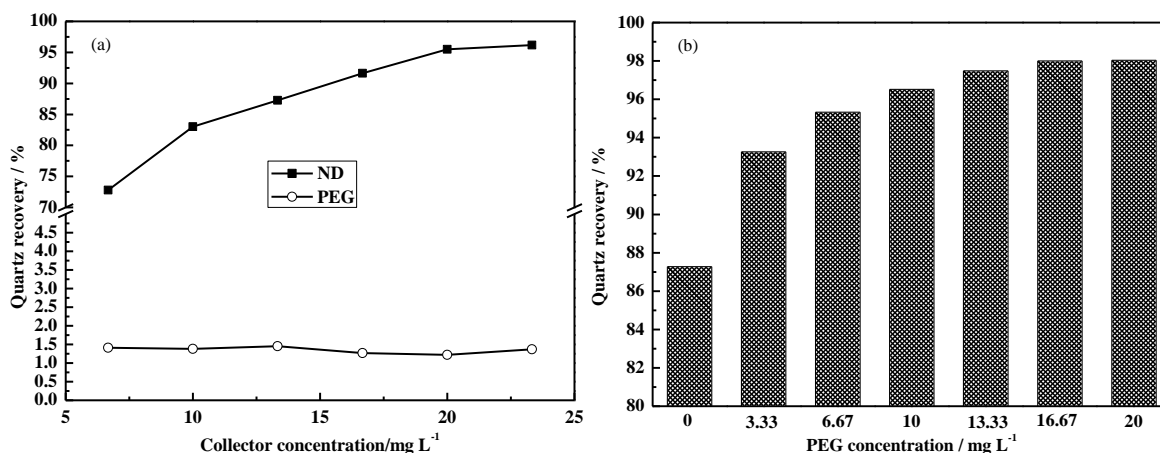


Figure 2. Flotation responses of pure quartz. (a) Effect of ND, PEG concentration; (b) Effect of ND/PEG mixture concentration.

Figure 2 (a) displayed the flotation of quartz when ND and PEG were used as collector separately. From the figure, it was observed that good flotation of quartz could be obtained when ND

was used as collector. And the flotation recovery of quartz was increasing with the increasing of ND concentration. High flotation recovery which was more than 95% could be obtained when ND concentration was above 20 mg L⁻¹. However, the recovery of quartz was independent of PEG concentration and little quartz was floated in the concentration range studied. Figure 2 (b) illustrated the effect of PEG concentration on flotation of quartz when ND concentration was 16.67mg L⁻¹. The result revealed increasing flotation recovery of quartz with the addition of PEG. The maximum flotation recovery was obtained when PEG concentration was equal to ND concentration.

ND, which belonged to cationic collector, had strong collecting performance on quartz due to electrostatic and hydrogen bonding adsorption [27]. Therefore, with the addition of ND concentration, flotation recovery of quartz was increasing dramatically. PEG was also preferentially adsorbed on quartz due to basic character of OH groups [28]. However, low hydrophobicity of quartz could be achieved because there were too many oxyethylenic groups in PEG [29]. Thus, lower floatability of quartz was achieved when PEG was used as collector. When PEG was added as additive into the flotation system of quartz with ND, co-adsorption of ND along with PEG had taken place on quartz surface, which resulted in the increase of flotation recovery of quartz.

3.1.2 Synthetic materials separation

Flotation studies with quartz showed that ND/PEG mixture had strong collecting ability to quartz, and the best collecting performance could be obtained when ND and PEG were mixed at a mass ratio of 1:1. Thereby, the affinity of this collector with quartz was further demonstrated by carrying out the flotation separation of synthetic mixture of hematite and quartz (Figure 3). In separation experiment, quartz and hematite were mixed at a mass proportion of 2:3.

The effect of slurry pH on flotation separation of the mixed sample at a starch concentration of 3.33mg L⁻¹ and a collector concentration of 33.33mg L⁻¹ was shown in Figure 3 (a). About this mixed hematite and quartz sample, the total Fe content of the feed was analyzed to be 41.9%. Figure 3(a) showed that with the increase of slurry pH, iron grade in concentrate tent to be increased slightly and then decreased sharply. However, iron recovery in concentrate was low at extreme acidic and alkaline pH value and showed a local maximum at pH around 7. Figure 3 (b) illustrated the effect of starch concentration on separation of this synthetic material when collector concentration was 33.33 mg L⁻¹ under the neutral condition. Results concluded from the figure displayed that iron recovery of concentrate gone rising and then kept steadily with the increasing of starch concentration. However, iron grade showed a small rising and then declining trend. The maximum iron recovery of 92.66% with 58.92% iron grade was obtained at starch concentration of 6.67 mg L⁻¹. Separation of mixed sample with 6.67mg L⁻¹ starch concentration under neutral condition at different collector concentrations was shown in Figure 3 (c). The results indicated that an increase in the collector concentration lead to increase of non-float concentrate iron grade, yet the iron recovery decreased correspondingly. At collector concentration of 20 mg L⁻¹ and 26.67 mg L⁻¹, iron grade of the concentrate was only 49.39% and 51.34%, respectively. However, at all other higher concentrations,

more than 55% iron grade could be obtained. The maximum iron grade of 58.92% with 92.66% iron recovery in concentrate was achieved when collector concentration was 33.33 mg L⁻¹.

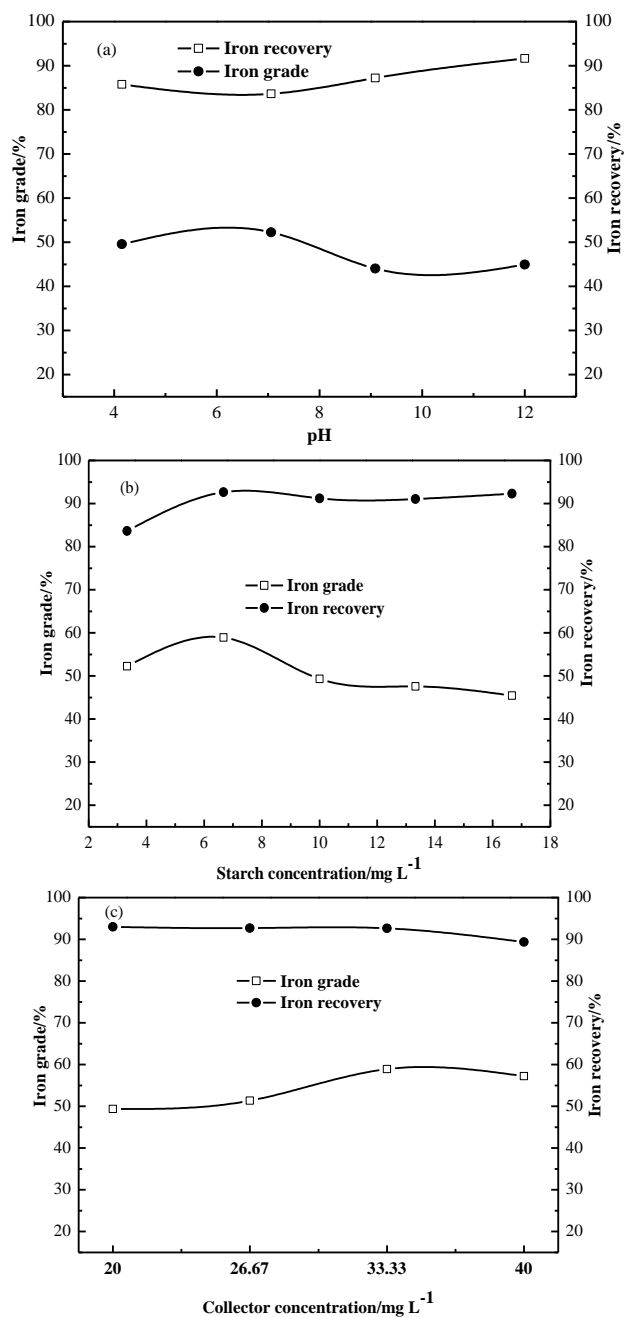


Figure 3. Effect of pH (a), starch concentration (b) and collector concentration (c) on flotation separation of quartz from hematite.

Under alkaline condition, desorption of PEG from quartz took place due to significant weakening of hydrogen bond between quartz and PEG chains [28]. Thus it was obvious that the concentration of quartz in the froth was declining in alkaline when slurry pH was higher than 7.0, resulted in the increasing of iron recovery and sharply reducing iron grade in concentrate.

3.2. Synergistic adsorption mechanism

3.2.1 Zeta potential measurements

The zeta-potential of a colloid, reflecting its surface charge, is important on its stability in the dispersion [30]. Zeta potentials of quartz in the absence and presence of ND and PEG in terms of pH were illustrated in Fig. 4. During experiment, ND or ND/PEG mixture at a mass ratio of 1:1 was added at a concentration of 33.33 mg L^{-1} .

Experiment results showed that zeta potentials of quartz, which were dependent of pH, were found to be negative in all pH values under research. And the isoelectric point (IEP) of quartz was less than 2.00. The addition of ND had strong influence on zeta potentials of quartz, the IEP of quartz increased to 3.11 greatly. Thus, a marked shift towards more positive zeta potentials was taken place, indicating the cationic ND molecules adsorption on quartz through electrostatic force [31]. In the presence of ND/PEG mixture, the IEP of quartz was increased to 6.21, revealing more positive zeta potentials of quartz were taken place than that in the presence of ND alone. This indicated an even stronger electrostatic adsorption between quartz and ND/PEG collector was produced. So flotation recovery of quartz was much higher when ND/PEG was used as collector than they were used individual at pH 6-7. However, when slurry pH was higher than 7.3, the value of negative charges on quartz surface after adsorbing ND/PEG was much higher than that adsorbing ND alone. This indicated that electrostatic adsorption between quartz and collector was weakened by PEG addition. Thus, declined quartz concentration in the froth was obtained, which agreed with the flotation results.

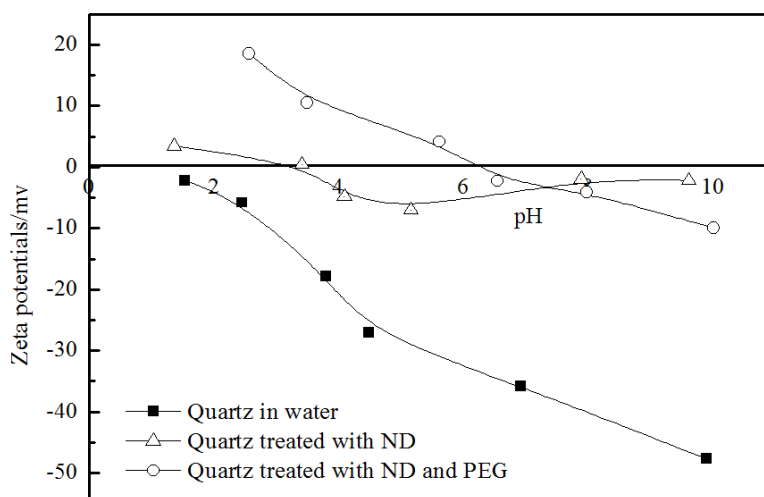


Figure 4. Zeta potentials of quartz in the absence and presence of ND and PEG.

3.2.2 FTIR studies

FTIR spectra of quartz and these conditioned with ND and mixture of ND/PEG at a mass ratio of 1:1 at pH 6–7 were given in Figure 5.

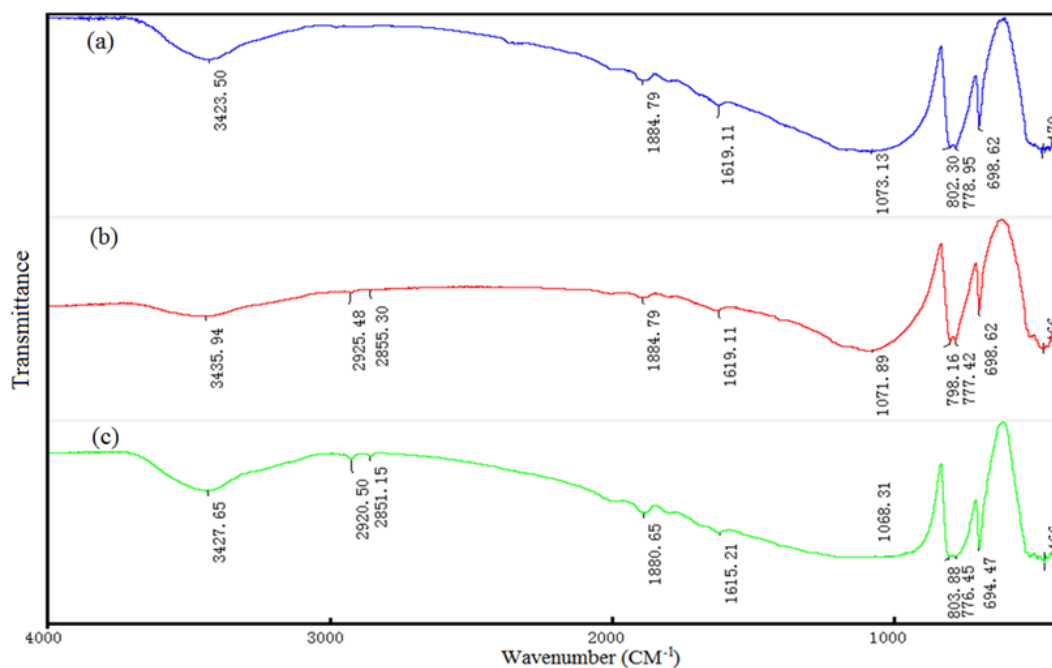


Figure 5. FTIR spectra of quartz in the absence and presence of ND and PEG at pH 6–7. (a) quartz; (b) quartz treated with ND; (c) quartz treated with ND/PEG.

In spectrum of quartz (Figure 5 (a)), the asymmetric stretching vibration of Si–O was characterized at 1073.13 cm^{-1} , the symmetric stretching vibration of Si–O was appeared at 802.98 and 778.95 cm^{-1} , and the blending vibration of Si–O was characterized at 470 cm^{-1} . In the figure, the adsorption peak of hydroxyl group was also visible, indicating the existence of crystallization water in quartz [32]. Compared with pure quartz spectrum, only weak –CH stretching peaks, that existed at 2925.48 cm^{-1} and 2855.30 cm^{-1} were observed in quartz after ND adsorption (Figure 5 (b)). The diagnostic peaks of quartz were not changed clearly but for red-shift, revealing weak physical adsorption of ND occurred on quartz surface [33]. After adsorbing with ND, the asymmetric stretching vibration and symmetric stretching vibration of Si–O in quartz varied from 1073.13 , 802.98 and 778.95 cm^{-1} to 1071.89 , 798.16 and 777.42 cm^{-1} , respectively, which indicated the hydrogen binding adsorption of collector on quartz surface [34]. When PEG was added, there was no new diagnostic peak generated on quartz surface, but the absorption peaks shifted to lower wave numbers. This demonstrated that PEG strengthened the hydrogen binding adsorption between quartz and ND.

3.2.3 SEM/EDS measurements

In order to characterize the surface morphology of quartz, a set of SEM/EDS probe analysis were implemented accordingly to investigate the type and distribution of ND and alcohol elements or their compounds on quartz surface. SEM image and microchemical maps of selected area of quartz (Figure 6) before and after being treated with ND/PEG (Figure 7) were displayed.

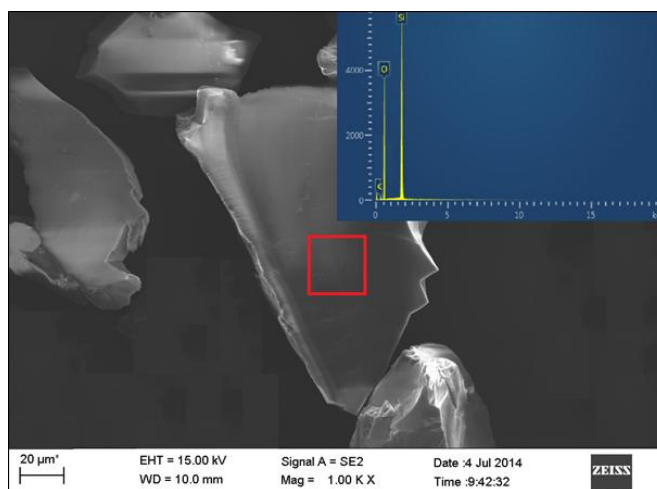


Figure 6. SEM image and microchemical maps of selected area of pure quartz.

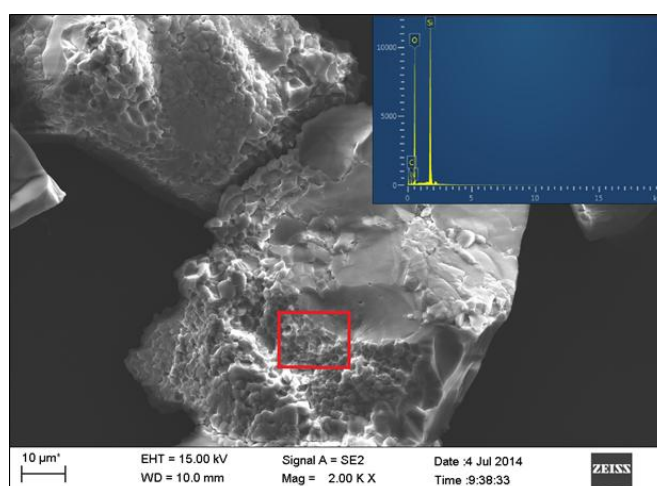


Figure 7. SEM image and microchemical maps of selected area of quartz treated with ND/PEG.

Figure 6 revealed that the surface of pure quartz displayed smoothly, and the oxygen and silicon elements distributed compactly and symmetrically on the surface. Compared with Figure 6, the surface of quartz after being treated with ND/PEG displayed a number of pores and holes. This revealed that corrosion had taken place on quartz surface. The microchemical maps of selected area indicated the existence of carbon and nitrogen elements clearly, which demonstrated that the collector had absorbed on quartz closely.

3.3. Molecular dynamics simulations

During molecular dynamics simulations, quartz surface like (0 0 1) is designated as the most stable one [35]. So, molecular dynamics simulations were performed by docking ND and ND/PEG mixtures on hydroxylated quartz (0 0 1) surface. MD simulations of the adsorption between quartz (0 0 1) surface and collector molecule in vacuum was performed in a simulation box (29.46 Å×29.46

Å×40.19 Å) with periodic boundary conditions. The corresponding adsorption energies for ND–quartz, PEG–quartz and ND/PEG (mass ratio 1:1)–quartz were shown in Table 2.

Table 2. Interaction energies (kcal/mol) of ND, PEG, ND/PEG mixture on quartz surface.

Molecules	ND	PEG	ND/PEG
ΔE	-4.97	-5.43	-33.10

Table 3. Hydrogen bond details for molecular adsorption of ND/PEG mixtures on hydroxylated quartz (0 0 1) surface.

H-bond	Formation	Bond length (Å)	Bond angle (°)
1	C-O...H-O-Si	1.96	160.40
2	O-H...O-Si	1.61	163.16
3	N-H...O-Si	2.01	149.24
4	C-N...H-O-Si	2.12	140.79

Results displayed in Table 2 showed that interaction energies for ND and PEG adsorption on quartz surface were calculated as -4.34 and -5.43 kcal mol⁻¹, respectively. This indicated that ND and PEG could adsorb on quartz individually, which had been confirmed by many researchers [27,28]. Moreover, far more negative interaction energy (-8.16 kcal mol⁻¹) could be obtained between ND/PEG mixture and quartz surface, which indicated more favorable interactions between quartz surface and ND/PEG mixture [36]. Thus, higher flotation recovery was achieved when ND and PEG were combining used.

The optimized configuration of molecular adsorption about ND, PEG and ND/PEG mixture over hydroxylated quartz (0 0 1) surface were shown in Figure 8. And also, the hydrogen bonding between ND/PEG mixture and hydroxylated quartz (0 0 1) surface were listed and presented by dotted lines. It could be concluded from the results that, the adsorption of collector, including ND, PEG and ND/PEG mixture, mainly occurred on silanol groups of hydroxylated quartz surface [15]. The adsorption of ND on silanol groups could be realized with the amino group hydrogen bonded to surface silanol (Figure 8 (a)). However, the hydrogen bond between PEG and quartz surface attributed to the oxyethylenic groups adsorption on surface silanol (Figure 8 (b)). When ND and PEG were added into the flotation system together, co-adsorptions between ND/PEG and quartz surface were taken place, and four types of hydrogen bonds, which were listed in Table 3, were formed between amino group of ND, hydroxyl group of alcohol and silanol on mineral surface. Additionally, when ND and PEG co-adsorbed on quartz surface, the adsorbed layer was closely packed due to hydrophobic interactions between the alkyl chains of ND and PEG, leading to increasing hydrophobicity [36] and maximum flotation recovery.

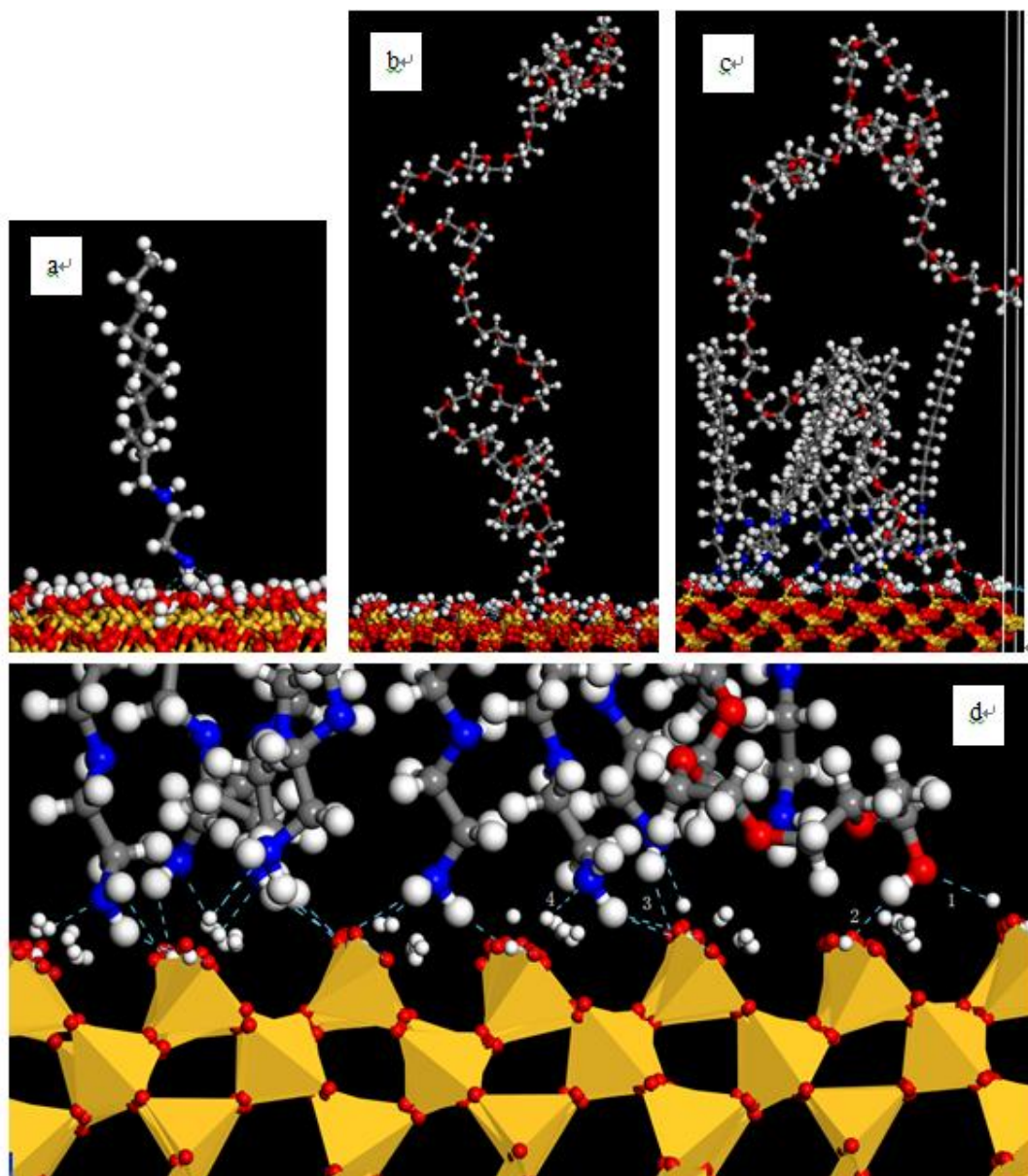


Figure 8. Interaction of hydroxylated quartz (0 0 1) surface with ND (a), PEG (b) and ND/PEG mixture (c) and the hydrogen bond between ND/PEG mixture and hydroxylated quartz (0 0 1) surface (d) (Oxygen atoms were shown in red; hydrogen atoms were shown in white; nitrogen atoms were shown in blue; and carbon atoms were shown in grey.).

4. CONCLUSION

Froth flotation results indicated that PEG had significant influence on quartz flotation using ND as collector. And quartz flotation recovery was enhanced with the addition of PEG at a particular ND concentration. The maximum flotation recovery of quartz was obtained when ND and PEG were mixed at a mass ratio of 1:1. Zeta potential measurements, FTIR analyses and SEM/EDS studies indicated that co-adsorption of PEG and ND on quartz surface was taken place. And the addition of

PEG strengthened the electrostatic and hydrogen bonding adsorption between ND and quartz, thus enhancing the flotation recovery. Molecular dynamics simulations show even more negative interaction energy could be obtained when ND and PEG co-adsorb on quartz surface. This revealed even stronger adsorption between ND/PEG mixture and quartz surface and resulted in higher quartz flotation recovery. Moreover, four types of hydrogen bonds were formed when ND and PEG co-adsorb on quartz surface. And the hydrophobic interactions between alkyl chains of ND and PEG lead to closely packed adsorbed layer and increasing the hydrophobicity of quartz surface.

ACKNOWLEDGEMENTS

This work was supported by the National Natural Science Foundation of China under Grant number 51374051; the Fundamental Research Funds for Central Universities under Grant number N130401008.

References

1. X.Q. Weng, G.J. Mei, T.T. Zhao, Y. Zhu, *Sep. Purif. Technol.*, 103 (2013) 187.
2. K.E. Waters, N.A. Rowson, X. Fan, J.J. Cilliers, *Asia-Pac. J. Chem. Eng.*, 4 (2009) 218.
3. S.S. Rath, H. Sahoo, B. Das, B.K. Mishra, *Miner. Eng.*, 69 (2014) 57.
4. M. Rudolph, U.A. Peuker, *Chem. Ing. Tech.*, 86 (2014) 865.
5. A. Liu, J.C. Fan, M.Q. Fan, *Int. J. Miner. Process.*, 134 (2015) 1.
6. M. Birinci, J.D. Miller, M. Sarıkaya, X.M. Wang, *Miner. Eng.*, 23 (2010) 813.
7. A.H. Englert, R.T. Rodrigues, J. Rubi, *Int. J. Miner. Process.*, 90 (2009) 27.
8. J. Kou, D. Tao, G. Xu, *Colloid. Surface. A*, 368 (2010) 75–83.
9. R.M. Papini, P.R.G. Brandao, A.E.C. Peres, *Miner. Metall. Process.*, 17 (2001) 1.
10. H. Sahoo, S.S. Rath, B. Das, *Sep. Purif. Technol.*, 136 (2014) 66.
11. H. Jiang, G.Y. Liu, Y.H. Hu, L.H. Xu, Y.W. Yu, *Int. J. Min. Sci. Technol.*, 23 (2013) 249.
12. K.C. Corin, J.C. Bezuidenhout, C.T. O'Connor, *Miner. Eng.*, 36–38 (2012) 100.
13. K. Hanumantha Rao, K.S.E. Forssberg, *Int. J. Miner. Process.*, 51 (1997) 67.
14. A. Vidyadhar, K. Hanumantha Rao, I.V. Chernyshova, *Colloid. Surface. A*, 214 (2003) 127.
15. A. Vidyadhar, K. Hanumantha Rao, I.V. Chernyshova, Pradip, K.S.E. Forssberg, *J. Colloid. Interf. Sci.*, 256 (2002) 59.
16. L.O. Filippov, I.V. Filippova, V.V. Severov, *Miner. Eng.*, 23 (2010) 91.
17. L.O. Filippov, A. Duverger, I.V. Filippov, H. Kasaini, J. Thiry, *Miner. Eng.*, 36–38 (2012) 314.
18. C. Klein, D. Harbottle, L. Alagha, Z.H. Xu, *Can. J. Chem. Eng.*, 91 (2013) 1427.
19. E. Burdukova, H.H. Li, D.J. Bradshaw, G.V. Franks, *Miner. Eng.*, 23 (2010) 921.
20. S. Pavlovic, P.R.G. Brandao, *Miner. Eng.*, 16 (2003) 1117.
21. D.A. Jones, W.A. Jordan, *J. Appl. Polym. Sci.*, 15 (1971) 2461.
22. W.G. Liu, D.Z. Wei, B.Y. Wang, P. Fang, X.H. Wang, B.Y. Cui, *T. Nonferr. Metal. Soc.*, 19 (2009) 1326.
23. C.E.G.R. Schaefer, R.J. Gilkes, R.B.A. Fernandes, *Geoderma.*, 123 (2004) 69.
24. L.H. Xu, Y.H. Hu, F.Q. Dong, Z.Y. Gao, H.Q. Wu, Z. Wang, *Appl. Surf. Sci.*, 321 (2014) 331.
25. K.F. Khaled, A.M. El-sherik, *Int. J. Electrochem. Sci.* 8 (2013) 10022.
26. Y.H. Hu, Z.Y. Gao, W. Sun, X.W. Liu, *Colloid. Surface. A*, 415 (2012) 439.
27. W.G. Liu, D.Z. Wei, B.Y. Cui, *T. Nonferr. Metal. Soc.*, 21 (2011) 1155.
28. P. Wang, M.Q. Yang, Z.X. Dong, S.Q. Bo, X.L. Jin, *Chem. Res. Chin. Univ.*, 29 (2013) 820.
29. J. Drzymala, E. Mielczarski, J.A. Mielczarski, *Colloid. Surface. A*, 308 (2007) 111.

30. W. Li, Y.D. Zheng, X.L. Fu, J. Peng, L.L. Ren, P.F. Wang, W.H. Song, *Int. J. Electrochem. Sci.* 8 (2013) 2164.
31. L.H. Xu, H.Q. Wu, F.Q. Dong, L. Wang, Z. Wang, J.H. Xiao, *Miner. Eng.*, 41 (2013) 41.
32. A. Vidyadhar, K. Hanumantha Rao, *J. Colloid. Interf. Sci.*, 306 (2007) 195.
33. L. Wang, W. Sun, Y.H. Hu, L.H. Xu, *Miner. Eng.*, 64 (2014) 44.
34. N.V. Chukanov, *Infrared spectra of mineral species*, Springer, New York, 2014.
35. S.S. Rath, H. Sahoo, B. Das, B.K. Mishra, *Miner. Eng.*, 69 (2014) 57.
36. L. Wang, Y.H. Hu, W. Sun, Y.S. Sun, *Appl. Surf. Sci.*, 327 (2015) 364.

© 2015 The Authors. Published by ESG (www.electrochemsci.org). This article is an open access article distributed under the terms and conditions of the Creative Commons Attribution license (<http://creativecommons.org/licenses/by/4.0/>).